RF Front-End Challenges for Joint Communication and Radar Sensing

Farhad Bozorgi, Padmanava Sen, André N. Barreto and Gerhard Fettweis
Barkhausen Institut, Dresden, Germany
farhad.bozorgi, padmanava.sen, andre.nollbarreto, gerhard.fettweis@barkhauseninstitut.org

***Abstract*—In this paper, radio-frequency (RF) hardware challenges for joint communication and radar sensing (JC&S) applications are studied. Different transceiver block requirements, namely amplifier and frequency synthesizers are described and compared for these two applications. The key concepts to efficiently meet the requirements of a joint system with single hardware are proposed. For the analysis, signal processing approach and waveforms that can satisfy requirements from both applications are considered.**

***Index Terms*—radar, sensing, RF, communications, hardware.**

I. Introduction

With growing consumer needs, wireless communications are reaching their throughput limits at sub-10 GHz bands and are already being extended to mm-Wave bands. This expansion may lead to spectrum constraints for radar applications but at the same time, creates an opportunity of context-aware communications systems with radar capability. Additionally, radar sensing for automotive applications is going to pave its way to be widely employed in civilian and individual daily applications, such as autonomous vehicles, drones, gesture recognition, health monitoring etc., which may overlap with the 5G New Radio (NR) frequency bands [1], [2]. Applications such as (autonomous) vehicular networks, as shown in Fig. 1, will employ both radar sensing and wireless communications. Conventionally, each service, radar and communication, has its own band and, consequently, its own hardware platform. A joint communication and radar sensing (JC&S) system integrates these two applications into one hardware platform and frequency band. This also allows the concept of radar as a service (RaaS), in which radar sensing can be offered as an additional service in wireless networks, sharing its radio resources, just as different communication services, such as machine-type communications (MTC), ultra-reliable low-latency communications (URLLC), mobile broadband (MBB), and localization are offered now.

Recently there has been an increased interest in joint radar and communication systems [3], [4]. The immediate advantages are visible in terms of spectrum sharing, while, at the same time, adding new functionalities to sensing and communication systems. It also creates the need and opportunity to design more cost- and power-efficient transceivers that can support such systems. There are several approaches to combine a radar system and a communication system. One can either use an existing radar system and add communication functionalities [5]. Otherwise, an existing communication system and waveform can be re-used to sense objects in a passive radar scenario [6], [7]. Finally, a waveform can be codesigned to actively support both radar and communications services. However, there is no commercial product available yet and the final realization of such a system will depend on the applications and cost-effectiveness of such a system. Fig. 1 shows one such application scenario in an automotive use case. The car has both active radar (sensing) and communication capability with an integrated transceiver TRX1. The base station on the other hand works primarily in the communication mode with passive radar capabilities. In this paper, we investigate some of the RF hardware challenges that we need to solve for an integrated communication and radar sensing platform.

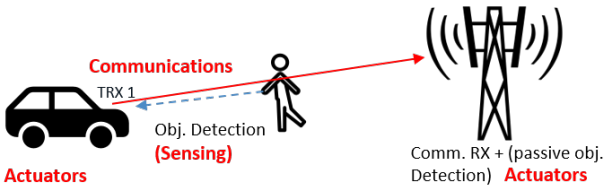

Fig. 1: Application of joint communication and sensing systems

Section II presents waveform and signal processing approach that has been considered in our analysis of the hardware challenges for a joint functional system. Section III gives details about the current state of the art of RF hardware in both communications and radio sensing. This section also highlights the hardware challenges while merging these applications in one device and possible solutions that can overcome the hardware challenges.

II. Waveforms and Signal Processing for JC&S

When selecting the waveform for a JC&S system, three main aspects must be taken into account. First, for an appropriate radar detection, the waveform must have good auto-correlation properties in both range and Doppler domains, which is represented by its

This work is financed by the Saxon State government out of the State budget approved by the Saxon State Parliament.

ambiguity function. Second, the waveform must allow the transmission of data, preferably with high spectral efficiency and/or high energy efficiency, represented by its bit-error-rate (BER) performance in relation to the signal-to-noise ratio (SNR). Third, the waveform must should be implementable with relatively low complexity for both radar and communications.

Currently, most waveform proposals for JC&S rely on either orthogonal frequency-division multiplexing (OFDM) or frequency-modulated continuous wave (FMCW). Both waveforms satisfy the first condition and can provide good radar detection and parameter estimation performances.

OFDM has been recently proposed in the literature for JC&S [8], and, whereas it excels in the second condition, it is arguably a poor choice if complexity is an issue, particularly for radar detection with high bandwidths, as a high-rate analog-to-digital converter (ADC) and full duplexing is required.

FMCW signals, also known as chirps, on the other hand have been extensively employed in different sorts of radar systems, mostly because of the low complexity of radar receivers using a mixer followed by a low-rate ADC, exploiting the concept of pulse compression. The radar self interference can be mitigated by adequate antenna separation and DC blocking. Regarding the data transmission, chirps can be modulated with low spectral efficiency, for instance, with FSK [5], or in phase and/or amplitude with moderate spectral efficiency [9].

Future wireless systems supporting JC&S will have to be flexible to provide either radar or communication services on demand, supporting also low-complexity low-energy transceivers. 6G systems will likely provide very high bandwidths, in the order of several GHZ. This will be beneficial for radar detection but will also be challenging for the hardware complexity, particularly for the ADC. Besides, on account of the high bandwidths, even moderate spectral efficiency values will still provide very high data rates.

Because of these issues, we believe that a modulated FMCW waveform can be a good candidate for future JC&S systems, allowing a flexible allocation of radio resources to radar and communication services. A JC&S frame can consist of a preamble using unmodulated and non-overlapping chirps, which can be used both for radar detection and channel estimation of the communications link. This preamble can be followed by a sequence of modulated chirps, possibly overlapping to increase the data rate. This is depicted in Fig. 2. The size of the preamble and of the communication part can be adapted, depending on the requirements of the radar and communication applications.

III. Hardware Implementation of JC&S

This section reviews the system and hardware requirements including different blocks in radar and communication systems and proposes possible solutions for JC&S. Fig. 3(a) shows the block diagram of a typical

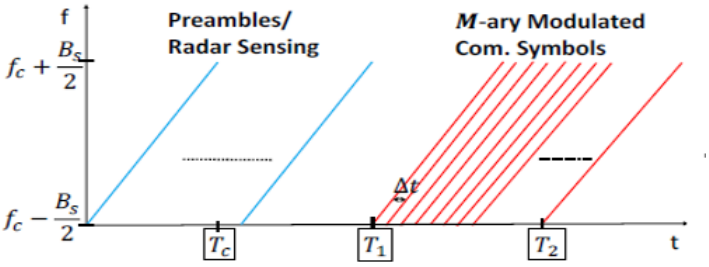

Fig. 2: Chirp-based waveform

direct-conversion transceiver (TRX), which is widely used in wireless communication integrated circuits (ICs). A typical FMCW radar system is shown in Fig. 3(b). It is employed for every range and velocity estimation of an object. Both systems share the same hardware sub-blocks, including voltage-controlled oscillator (VCO) or phased-locked loop (PLL), low-noise amplifier (LNA), power amplifier (PA), frequency mixers, analog-to-digital converter (ADC), filters etc. The required performance can vary for each application. However, when it comes to integrated JC&S, the target specifications of each block have to satisfy both the radar and communications systems. Design and realization of the main blocks that are more challenging in JC&S, including VCO/PLL, LNA and PAs, will be surveyed individually.

A. VCO/PLL

In an ideal oscillator, the output signal has a constant period expressed by $x(t) = A\cos(\omega_c t + \Phi_0)$ in which the

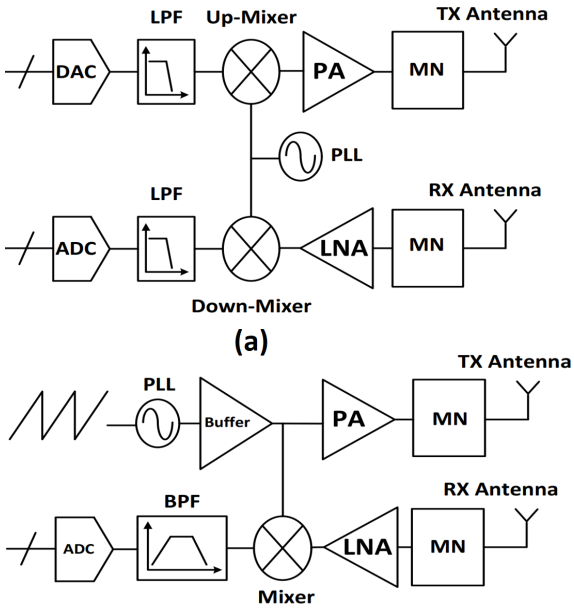

Fig. 3: Typical (a) communication and (b) Radar Transceiver block diagram.

spectrum can be represented by an impulse at the carrier angular frequency ω_c (Fig. 4(a)). However, due to the phase noise $n(t)$, it varies as $x(t) = A\cos(\omega_c t + \Phi_0 + n(t))$. The instantaneous frequency varies randomly and it can be proved [10] that the spectrum will be "skirt shaped" [11] as shown in Fig. 4(b). Hence, in FMCW radars where the chirp is generated by a VCO in TX, the output signal will have a phase noise. Since the RX receives the delayed replica from an object, phase noise will be present in the received signal. When RX and TX are mixed, the IF signal spectrum will no longer be a single impulse and its phase and frequency will also change randomly. Consequently, it will affect the precision of range and velocity detection of the FMCW radar. At the receiver, the incoming signal is mixed and down-converted by VCO to the Intermediate Frequencies (IF). Considering the IF spectrum in Fig. 4(c), at the offset of $\Delta\omega$ from center IF frequency, ω_{IF}, a single tone noise, a, is added. Then, corresponding phase change in time domain will be expressed as

$$x(t) = A\cos\left(\omega_{IF}t + \Phi_0 - \frac{a}{A}\sin(\Delta\omega t)\right). \quad (1)$$

Doing the same for all frequencies below the skirts, the total IF phase shift can be expressed as

$$x(t) = A\cos\left(\omega_{IF}t + \Phi_0 - \sum\frac{a_k}{A}\sin(\Delta\omega_k.t)\right). \quad (2)$$

where $\frac{a_k}{A}$ represents the phase noise of the VCO at $\Delta\omega_k$ offset from the center frequency of the transmitted signal. The corresponding phase change in the time domain is exemplified in Fig. 4(d). For the FMCW radar, the distance d and velocity v are calculated from the frequency and phase, respectively, as

$$d = \frac{c.\omega_{IF}}{2S} \quad (3)$$

$$v = \frac{\lambda_C.\Phi_0}{4\pi.T_C}, \quad (4)$$

where c is the free-space speed of electromagnetic wave and $S = \frac{BW}{T_C}$ the slope of the chirp, with BW the chirp sweep bandwidth and T_C the chirp duration. T_C is the inter-chirp interval, and λ_C is the wavelength of the carrier signal.

As a result, considering 2, the range and velocity errors due to the phase noise can be expressed, respectively, as

$$\Delta d = \frac{c}{2S}\sum\frac{a_k(\Delta\omega_k)}{A}\Delta\omega_k\cos(\Delta\omega_k.T_{ToF},) \quad (5)$$

$$\Delta v = \frac{\lambda_C}{4\pi.T_C}\sum\frac{a_k(\Delta\omega_k)}{A}\sin(\Delta\omega_k.T_{ToF}), \quad (6)$$

where T_{ToF} is the time of flight (ToF) of radar signal from transmitter to receiver. In short- and medium-range radars, T_{ToF} is relatively small (in the order of tens of nanoseconds). Hence, in (5) and (6), the cosine and sine terms will be close to 1 and 0, respectively. Therefore, the velocity error due to phase noise will be negligible and the distance error can be represented as

$$\Delta d = \frac{c}{2S}\sum\frac{a_k(\Delta\omega_k)}{A}\Delta\omega_k. \quad (7)$$

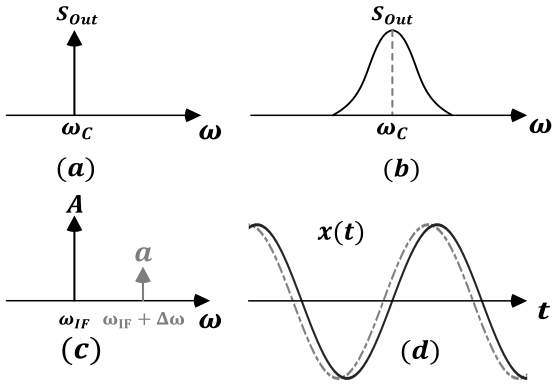

Fig. 4: Output spectrum of (a) an Ideal VCO and (b) VCO with phase noise. (c) received-signal phase noise spectrum (d) translation of phase noise into time. [11]

TABLE I: Comparison between Communication and Radar VCO specs.

Comm.	Freq. (GHz)	Phase Noise @1MHz (dBC/Hz)	Tuning Range (GHz)
[17]	73	-93.5	7.15
[15]	75	-100	11.25
[18]	83.4	-91.2	8
Radar System	**Freq. (GHz)**	**Phase Noise @1MHz (dBC/Hz))**	**Chirp BW (GHz)**
[19]	78	-85	0.6
[20]	78.4	-87.4	4
[21]	78.5	-100	5

It can be deduced from (5) and (6) that the distance error due to phase noise depends on the chirp slope and on the integral of the normalized signal spectrum over frequency.

On the other hand, due to the existence of strong interferers, the VCO phase noise is crucial to avoid the interferers that can ruin the in-band data. Various techniques such as class C VCO [12], $1/f$ noise reduction rejection [13] and class F [14], multicore VCO [15], among others, have been proposed to reduce the phase noise, which can also be applicable to the radar. Table I shows the VCO/PLL phase noise in recent works for both communication and radar systems. Generally, at mm-wave frequencies communication transceivers should have a wider VCO/PLL tuning range to address the high-throughput data. Thus, when used in JC&S systems, radar system can benefit from a wider chirp bandwidth and, subsequently, a higher resolution.

However, VCO non-linearity is an issue that can affect the range resolution as well. Generally, in mm-wave frequencies, the main components of a VCO, such as varactors and inductors, are highly non-linear, particularly for a wide tuning range. As shown in Fig. 5, the VCO non-linearity manifests itself as non-linearity a chirp waveform. Fig. 5 shows that one solution is to pre-distort the control voltage based on the VCO frequency profile

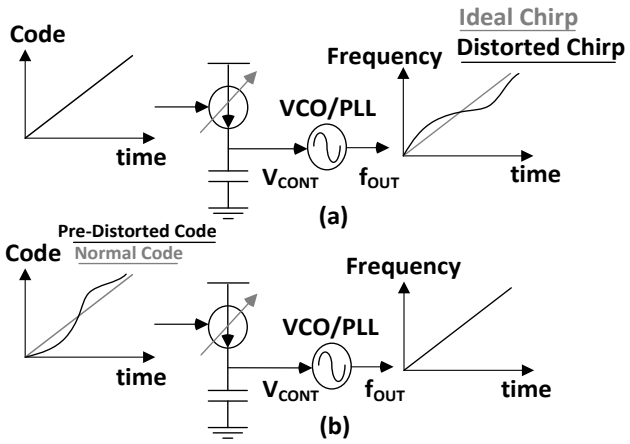

Fig. 5: (a) Non Linearity in VCO and Consequently Chirp output. (b) Applying Predistortion to VCO Control Voltage (V_{CONT}) to Compensate the Chirp Non-Linearity.

[16]. Nevertheless, it requires tuning under temperature variations. Typically, in communication transceivers, the VCO is put into a PLL/synthesizer-loop. In this way, also for the radar system, the chirp can be linearized. On the other hand, as the frequency increases, achieving low noise performance with the frequency synthesizers will be more challenging particularly in wireless communication transceivers. An interesting alternative is to design a VCO and PLL at lower frequencies, then up-convert the signal to a higher band by means of frequency multipliers [22]. The use of sub-sampling PLL (SSPLL) technique is another approach towards low-power PLLs [23].

B. Power Amplifiers

Broadband PAs are on high demand for high throughput transmitters in wireless communications, as well as in high resolution radars. Normally PAs are power hungry since they must deliver a high amount of power to be emitted by the antenna. As shown in Fig. 6, a parameter called power-added efficiency (PAE) is defined to characterize the efficiency of a PA according to the input power (P_{in}), delivered output power to the antenna load (P_{out}) and supply power (P_{supply}). The PAE can be defined as [24]

$$PAE = \frac{P_{out} - P_{in}}{P_{Supply}} = \left(1 - \frac{1}{G_p}\right)\frac{P_{out}}{P_{supply}}, \tag{8}$$

where G_p is the power gain of a PA. The higher the gain, the better is the power efficiency, but the gain-bandwidth product is a constant value, which depends on the silicon technology. Thus, for a given power, bandwidth trades with gain and efficiency [24]. One major problem in a mm-wave PA is the low efficiency at 6 dB back-off (when PA is working quite below the maximum output power), at which it is in the range of 1 to 3%. Class-B PAs can increase the efficiency; however, they have linearity issues. Wireless communication protocols must obey specific masks for

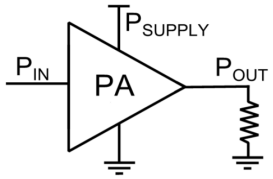

Fig. 6: Power Added Efficiency definition. [24]

TABLE II: Comparison between Communication and Radar PA Specs.

Comm.	Center Freq. (GHz)	$OP1dB$ (dBm)	max. PAE (%)	BW (GHz)
[25]	80	20.5	22	15
[28]	76	22.3	12.4	12
[29]	73	17.8	19.3	7.6
Radar	**Center Freq. (GHz)**	**P_{SAT} (dBm)**	**max PAE (%)**	**Chirp BW (GHz)**
[21]	78.5	18	NA	5
[30]	78.5	10.8	NA	4
[20]	78.5	13.4	NA	4

spectral regrowth that would take PA linearity into account. 1 dB output compression point (OP1dB), 3rd-order inter-modulation (IM3) and AM-PM conversion are the main linearity parameters in PA design. Many techniques have been proposed for the RF and mm-wave PAs to address the efficiency and linearity constraints, such as class AB [25], class E [26], Doherty [27] and current-clamping PAs. In radar systems, the minimum PA output depends on the link budget from TX to RX, which will be defined later in this section.

As a result, the PA characteristics in JC&S system must satisfy the linearity and PAE requirements to meet the wireless communications standards, while maintaining the minimum power required for the radar sensing systems to meet object detection requirements. Table II, summarizes the state-of-the-art PA characteristics in both systems. The PAs designed for high Peak to Average Power Ratio (PAPR) modulations in wireless communication are required to work mostly at 6dB back-off from their OP1dB to maintain the linearity. Hence, the higher OP1dB (which could be achieved by power combining), the more linear is the wireless communication TX. On the contrary, a radar TX typically works at maximum output power (close to P_{SAT}). The numbers in Table II show that the OP1dB in communication PAs are normally higher than the P_{SAT} in radar PA and the same applies also for the PA BW. Therefore, the main PA characteristics for communication can address the needs for radar TX.

C. Low-noise amplifiers

In classical radar and wireless communication systems, the LNA is the first analog front-end stage, which should match the antenna at the input while simultaneously

TABLE III: Comparison between Communication and Radar LNA Specs.

Comm.	Freq. (GHz)	NF	IP1dB (dBm)	BW (GHz)
[32]	75.1	8.3-10	-25	12.5
[33]	79	6.2-7	-32.5	8
[34]	75	7.3-9.1	-30.7	27.5
Radar	**Center Freq. (GHz)**	**NF**	**IP1dB (dBm)**	**Chirp BW (GHz)**
[21]	78.5	10-11	1	5
[30]	78.5	18	-7	4
[20]	78.5	15.3	-8.5	4

amplifying the weakened signal at the RX input. Since LNA is the first stage in RX, its noise can highly affect the overall noise figure and sensitivity of the receiver. For each wireless communication application, there are specific requirements on the maximum sensitivity level for the RX. For the radar system, the RX signal-to-noise ratio (SNR) can be expressed as

$$SNR = \frac{P_T G_{TX} \sigma G_{RX} \lambda^2 T_{measure}}{(4\pi)^3 d^4 kT(NF)}, \tag{9}$$

where P_T is the transmitted signal power, G_{TX} and G_{RX} the gain of antenna at TX and RX side, σ the reflection cross section of the target, λ the wavelength of the transmitted signal, k the Boltzmann constant, T the temperature, $T_{measure}$ the measurement time, NF the noise figure of the LNA and d is the distance of the object. The maximum distance that can be measured by radar depends on the minimum SNR (SNR_{min}) as

$$d_{\max} = \left(\frac{P_T G_{TX} \sigma G_{RX} \lambda^2 T_{measure}}{(4\pi)^3 kT(NF)(SNR_{\min})} \right)^{\frac{1}{4}}. \tag{10}$$

The value of SNR_{min} in Eq. 10 can be chosen on the basis of trade-off between the probability of missed detection (higher SNR_{min}) and the false-alarm probability (lower SNR_{min}). The LNA with lower NF proposed in the literature for mm-wave frequencies [31] can contribute to higher detection range of a radar. Also, it can help to reduce the bit error rate (BER) in wireless communications. The NF parameters for both radar and communication RX for recent state-of-the-art receivers are reported in Table III.

Unlike communication systems, the radar system has to work in full-duplex mode where the TX and RX would simultaneously. The leakage from TX to RX can saturate the LNA. Therefore, the linearity parameter in radar is more vita,l as the numbers in Table III states.

D. Future JC&S Systems

Since both TX and RX in radar/communication are implemented on the same chip, the leakage from TX to RX would be problematic. Given that TX propagates a quite higher power to the antenna, even a small amount of leakage by the shared substrate to RX can desensitize the LNA. One solution is to do the up-conversion and down-conversion at two different frequencies. It can be used for communication systems but not for radar. Additionally, even in communication systems, where spectrum digestion is the main issue, this approach occupies twice the bandwidth, which is not desirable. Employing a duplexer is a known approach that provides enough isolation between TX/RX [35], which also can be used in JC&S with additional overheads.

To circumvent the leakage in the radar TRX, as well as the excessive power consumption of the LNA with matching network in wireless MIMO RX, mixer-first receivers seem a suitable alternative for JC&S. Then, the question is how to manage the noise level at the RX input. The use of MIMO transceivers and beamforming techniques is going to be dominant for the next generation of communication such as 5G [36]. In MIMO transceivers, the noise requirement is more relaxed as the number of antennas are increased. Conventional mm-wave LNAs in RX require wideband inter-stage matching networks at the cost of significant area and power consumption [37]. However, recent works have tried to eliminate the need for an LNA in RX, as shown in Fig. 7(a). This approach is named as mixer-first receivers.

Fig. 7(b) shows the mixer-first structure for a radar working at 170 GHz [38]. At such high frequencies, reaching reasonable performance (in terms of noise figure, gain, and bandwidth) is challenging for the LNA. Therefore, mixer-first topologies are used at the expense of higher noise power at the input. This would deteriorate the RX NF, and according to (10) the maximum detectable distance is decreased. As a result, requiring large data throughput

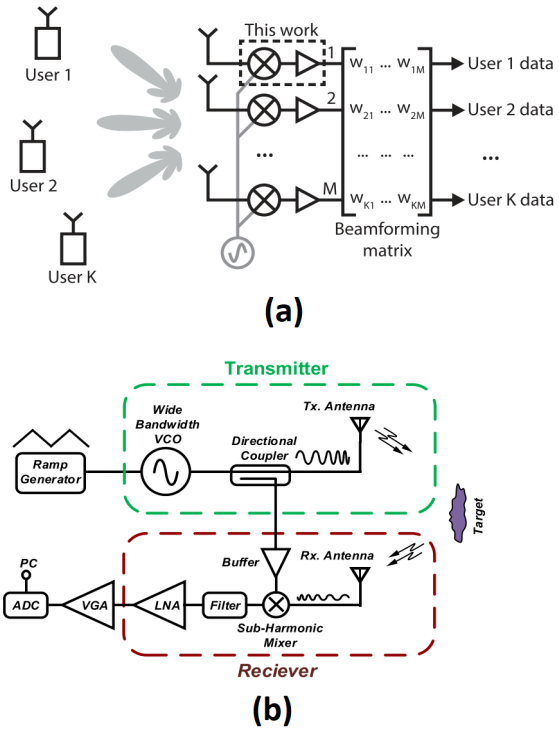

Fig. 7: Mixer-first structures in (a) a MIMO Receiver [37] and (b) 170GHz FMCW Imaging Radar [38].

in near future mandates JC&S systems to use MIMO TRXs. Consequently, a mixer-first RX would be a proper approach for hardware implementation of JC&S systems.

IV. Conclusion

In this paper, RF front-end challenges for joint communication and radar sensing (JC&S) applications are analyzed and possible ways to converge the requirements in a single transceiver are proposed. Different building blocks of a typical transceiver, namely amplifiers and frequency synthesizers, considering a chirp-based waveform are extensively studied to build a joint system.

References

[1] O. B. Akan and M. Arik, "Internet of Radars: Sensing versus Sending with Joint Radar-Communications," in IEEE Communications Magazine, vol. 58, no. 9, pp. 13-19, September 2020.

[2] F. Liu et al., "Joint Radar and Communication Design: Applications, State-of-the-Art, and the Road Ahead," in IEEE Transactions on Communications, vol. 68, no. 6, pp. 3834-3862, June 2020.

[3] de Lima et al., "6G White Paper on Localization and Sensing [White paper]", (6G Research Visions, No. 12), University of Oulu, 2020

[4] B. Paul et al., "Survey of RF Communications and Sensing Convergence Research," in IEEE Access, vol. 5, pp. 252-270, 2017.

[5] S. Dwivedi et al., "Target Detection in Joint Frequency Modulated Continuous Wave (FMCW) Radar-Communication System," 16th International Symposium on Wireless Communication Systems (ISWCS), Oulu, 2019, pp. 277-282.

[6] P. Kumari J. Choi N. González-Prelcic R.W. Heath "IEEE 802.11 ad-based radar: An approach to joint vehicular communication-radar system" IEEE Trans. on Vehicular Technology vol. 67 no. 4 pp. 3012-3027,April 2018.

[7] R. S. Thoma et al., "Cooperative Passive Coherent Location: A Promising 5G Service to Support Road Safety," in IEEE Communications Magazine, vol. 57, no. 9, pp. 86-92, September 2019.

[8] C. Sturm and W. Wiesbeck, "Waveform Design and Signal Processing Aspects for Fusion of Wireless Communications and Radar Sensing," in Proceedings of the IEEE, vol. 99, no. 7, pp. 1236-1259, July 2011.

[9] T. M. Pham et al., "Efficient Communications for Overlapped Chirp-Based Systems," in IEEE Wireless Communications Letters, vol. 9, no. 12, pp. 2202-2206, Dec. 2020.

[10] A. Hajimiri and T. H. Lee, "A general theory of phase noise in electrical oscillators," in IEEE Journal of Solid-State Circuits, vol. 33, no. 2, pp. 179-194, Feb. 1998.

[11] Behzad Razavi, "RF microelectronics", Vol. 2. New York: Prentice Hall, 2012.

[12] A. Mazzanti and P. Andreani, "Class-C Harmonic CMOS VCOs, With a General Result on Phase Noise," in IEEE Journal of Solid-State Circuits, vol. 43, no. 12, pp. 2716-2729, Dec. 2008.

[13] M. Shahmohammadi et al., "A 1/f Noise Upconversion Reduction Technique for Voltage-Biased RF CMOS Oscillators," in IEEE Journal of Solid-State Circuits, vol. 51, no. 11, pp. 2610-2624, Nov. 2016.

[14] M. Babaie and R. B. Staszewski, "A Class-F CMOS Oscillator," in IEEE Journal of Solid-State Circuits, vol. 48, no. 12, pp. 3120-3133, Dec. 2013.

[15] L. Iotti et al., "Insights Into Phase-Noise Scaling in Switch-Coupled Multi-Core LC VCOs for E-Band Adaptive Modulation Links," in IEEE Journal of Solid-State Circuits, vol. 52, no. 7, pp. 1703-1718, July 2017.

[16] P. T. Renukaswamy et al., "17.7 A 12mW 10GHz FMCW PLL Based on an Integrating DAC with 90kHz rms Frequency Error for 23MHz/µs Slope and 1.2GHz Chirp Bandwidth," 2020 IEEE International Solid-State Circuits Conference - (ISSCC), San Francisco, CA, USA, 2020.

[17] M. Vigilante and P. Reynaert, "Analysis and Design of an E-Band Transformer-Coupled Low-Noise Quadrature VCO in 28-nm CMOS," in IEEE Transactions on Microwave Theory and Techniques, vol. 64, no. 4, pp. 1122-1132, April 2016.

[18] J. Xu et al., "A 79.1–87.2 GHz 5.7-mW VCO With Complementary Distributed Resonant Tank in 45-nm SOI CMOS," in IEEE Microwave and Wireless Components Letters, vol. 29, no. 7, pp. 477-479, July 2019.

[19] T. Mitomo et al., "A 77 GHz 90 nm CMOS Transceiver for FMCW Radar Applications," in IEEE Journal of Solid-State Circuits, vol. 45, no. 4, pp. 928-937, April 2010.

[20] T. Ma et al., "A CMOS 76–81-GHz 2-TX 3-RX FMCW Radar Transceiver Based on Mixed-Mode PLL Chirp Generator," in IEEE Journal of Solid-State Circuits, vol. 55, no. 2, pp. 233-248, Feb. 2020.

[21] T. Fujibayashi et al., "A 76- to 81-GHz Multi-Channel Radar Transceiver," in IEEE Journal of Solid-State Circuits, vol. 52, no. 9, pp. 2226-2241, Sept. 2017.

[22] M. Bassi et al., "A 39-GHz Frequency Tripler With >40-dBc Harmonic Rejection for 5G Communication Systems in 28-nm Bulk CMOS," in IEEE Solid-State Circuits Letters, vol. 2, no. 9, pp. 107-110, Sept. 2019.

[23] X. Gao et al., "A Low Noise Sub-Sampling PLL in Which Divider Noise is Eliminated and PD/CP Noise is Not Multiplied by N2 ," in IEEE Journal of Solid-State Circuits, vol. 44, no. 12, pp. 3253-3263, Dec. 2009.

[24] J. Zhao et al., "2.6 A SiGe BiCMOS E-band power amplifier with 22% PAE at 18dBm OP1dB and 8.5% at 6dB back-off leveraging current clamping in a common-base stage," 2017 IEEE International Solid-State Circuits Conference (ISSCC), San Francisco, CA, 2017.

[25] E. Rahimi et al., "High-Efficiency SiGe-BiCMOS *E* -Band Power Amplifiers Exploiting Current Clamping in the Common-Base Stage," in IEEE Journal of Solid-State Circuits, vol. 54, no. 8, pp. 2175-2185, Aug. 2019.

[26] K. Datta and H. Hashemi, "Watt-Level mm-Wave Power Amplification With Dynamic Load Modulation in a SiGe HBT Digital Power Amplifier," in IEEE Journal of Solid-State Circuits, vol. 52, no. 2, pp. 371-388, Feb. 2017.

[27] F. Wang, T. Li, S. Hu and H. Wang, "A Super-Resolution Mixed-Signal Doherty Power Amplifier for Simultaneous Linearity and Efficiency Enhancement," in IEEE Journal of Solid-State Circuits, vol. 54, no. 12, pp. 3421-3436, Dec. 2019.

[28] H. Lin and G. M. Rebeiz, "A 70–80-GHz SiGe Amplifier With Peak Output Power of 27.3 dBm," in IEEE Transactions on Microwave Theory and Techniques, vol. 64, no. 7, pp. 2039-2049, July 2016.

[29] D. Zhao and P. Reynaert, "A 40-nm CMOS E-Band 4-Way Power Amplifier With Neutralized Bootstrapped Cascode Amplifier and Optimum Passive Circuits," in IEEE Transactions on Microwave Theory and Techniques, vol. 63, no. 12, pp. 4083-4089, Dec. 2015.

[30] B. P. Ginsburg et al., "A multimode 76-to-81GHz automotive radar transceiver with autonomous monitoring," 2018 IEEE International Solid - State Circuits Conference - (ISSCC), San Francisco, CA, 2018.

[31] L. Gao et al., "Design of E- and W-Band Low-Noise Amplifiers in 22-nm CMOS FD-SOI," in IEEE Transactions on Microwave Theory and Techniques, vol. 68, no. 1, pp. 132-143, Jan. 2020.

[32] M. Vigilante and P. Reynaert, "A Coupled-RTWO-Based Subharmonic Receiver Front End for 5G *E* -Band Backhaul Links in 28-nm Bulk CMOS," in IEEE Journal of Solid-State Circuits, vol. 53, no. 10, pp. 2927-2938, Oct. 2018.

[33] D. Guermandi et al., "19.7 A 79GHz binary phase-modulated continuous-wave radar transceiver with TX-to-RX spillover cancellation in 28nm CMOS," 2015 IEEE International Solid-State Circuits Conference - (ISSCC) Digest of Technical Papers, San Francisco, CA, 2015.

[34] M. Vigilante and P. Reynaert, "On the Design of Wideband Transformer-Based Fourth Order Matching Networks for *E* -Band Receivers in 28-nm CMOS," in IEEE Journal of Solid-State Circuits, vol. 52, no. 8, pp. 2071-2082, Aug. 2017.

[35] K. Y. Son et al., "A Dual-Band CMOS Tunable Duplexer Employing a Switchable Autotransformer for Highly Integrated RF Front Ends," in IEEE Microwave and Wireless Components Letters, vol. 29, no. 7, pp. 495-497, July 2019.

[36] M. Hashemi et al., "Out-of-Band Millimeter Wave Beamforming and Communications to Achieve Low Latency and High Energy Efficiency in 5G Systems," in IEEE Transactions on Communications, vol. 66, no. 2, pp. 875-888, Feb. 2018.

[37] L. Iotti et al., "A Low-Power 70–100-GHz Mixer-First RX Leveraging Frequency-Translational Feedback," in IEEE Journal of Solid-State Circuits, vol. 55, no. 8, pp. 2043-2054, Aug. 2020.

[38] A. Mostajeran et al., "A 170-GHz Fully Integrated Single-Chip FMCW Imaging Radar with 3-D Imaging Capability," in IEEE Journal of Solid-State Circuits, vol. 52, no. 10, pp. 2721-2734, Oct. 2017.